*Korean J. Chem. Eng.*, **27**(5), 1462-1468 (2010)
DOI: 10.1007/s11814-010-0252-1

# Enhanced photoelectric efficiency by surface modification of $TiO_2$ thin film using various acidic species

**Harim Jeong, Yeji Lee, Youngmi Kim, and Misook Kang†**

Department of Chemistry, College of Science, Yeungnam University, Gyeongsan, Gyeongbuk 712-749, Korea
(*Received 16 December 2009 • accepted 19 May 2010*)

**Abstract**−This study examined the photoelectric conversion efficiency of the dye-sensitized solar cell (DSSC) when the surface of a nanometer-sized $TiO_2$ film, which was prepared using the solvothermal method, was modified by five acid compounds. The $TiO_2$ film exhibited an anatase structure with an average particle size in the range of 10-15 nm, and the maximum absorption band was shown in the UV-visible spectrum around 360 nm. The surface colors of the carboxylic acid-modified $TiO_2$ films were changed to light or dark with differing energy conversion efficiencies. Particularly, the conversion efficiency was considerably enhanced from approximately 6.25% for the non-modified $TiO_2$ film to approximately 7.50% for the film treated by acetic acid of 1.0 mole, with the N719 dye under 100 $mW/cm^2$ of simulated sunlight. FT-IR analysis of the films after N719 dye adsorption confirmed that the IR spectrum of the modified $TiO_2$ showed a sharp and strong band at 500 $cm^{-1}$, which was assigned to a metal-O bond, due to the formation of a new Ti-O bond between the O of $COO^-$ and the Ti atom, which was relatively weaker in the non-modified $TiO_2$. Furthermore, these results were in agreement with an electrostatic force microscopy (EFM) study showing that the electrons were transferred rapidly to the surface of the acetic acid-modified $TiO_2$ film, compared with that on the non-modified $TiO_2$ film.

Key words: DSSC, Carboxylic Acids, Enhancement of Photovoltaic Efficiency, EFM, FT-IR

## INTRODUCTION

Dye-sensitized solar cells (DSSC) have been studied extensively due to their low cost, less toxic manufacturing, easy scale-up, light weight and potential use of flexible panels, compared to conventional p-n junction devices [1-3]. DSSC consists of a sensitizing dye, transparent conducting substrates (F-doped tin oxide), nanometer-sized $TiO_2$ film, iodide electrolyte, and counter electrode (Pt or carbon) [4,5]. When a dye molecule absorbs light, electrons on the highest occupied molecular orbital (HOMO) are excited to an electronically excited state: the lowest unoccupied molecular orbital (LUMO). When a dye molecule absorbs light, it leads to the excitation of electrons on the highest occupied molecular orbital (HOMO) to an electronically excited state, the lowest unoccupied molecular orbital (LUMO). The excited dye molecule injects an electron into the conducting band of the $TiO_2$ film. The oxidized dye is restored by electron donation from the reducing ions in the electrolyte, usually an organic solvent containing a redox system. The donated electron is in turn regenerated by the reduction of conjugated ions in electrolytes. The circuit is completed by electron migration through an external load [6-9].

The following four factors influence the photoelectric performance of the DSSC. 1) The electron transfer time from the dye to $TiO_2$ electrons must be shorter than the recombination time between the generated electrons and holes in the dye. 2) The conduction band of the $TiO_2$ semiconductor should be higher than the LUMO energy of the dye. 3) The electrons on the conduction band of $TiO_2$ should not be combined with the oxidation-reduction electrolytes. 4) The dye molecule should not decompose during the passage of electrons from the electrolyte, so that this reaction has a strong influence on the cell lifetime. The most important factor for increasing the DSSC efficiency is the strong interaction between the dye and the $TiO_2$. If the dye molecules are stably coordinated onto the surface of the $TiO_2$ film in structural or energy divisions, the electrons generated at the LUMO of the dye can be passed to the surface of $TiO_2$ without the partial loss of any electrons, which eventually raises the photoelectric efficiency. Additionally, the perfect combination of the dye on the $TiO_2$ surface can depress the by-reaction between the $TiO_2$ surface and the electrolytes, thereby increasing the cell life. However, no research has yet been conducted on modification of the thin $TiO_2$ film surface in order to improve the photovoltaic efficiency in DSSC.

Therefore, this study tried to enhance the photoelectric conversion efficiency of DSSC by modifying the surface of the nanometer-sized $TiO_2$ film, which was prepared using the solvothermal method, by five acid compounds with carboxyl group. The synthesized sample was characterized by X-ray diffraction (XRD), transmission electron microscopy (TEM), UV-visible and Fourier transform infrared (FT-IR) spectroscopy, and electrostatic force microscopy (EFM) analysis. The photovoltaic performance of six types of $TiO_2$/dye (N719) solar cell was evaluated from the overall conversion efficiency, fill factor (FF), open-circuit voltage ($V_{oc}$) and short-circuit current density ($J_{sc}$).

## EXPERIMENTAL

### 1. Preparation and Characteristics of Nanometer-sized $TiO_2$

$TiO_2$ particles were prepared using the solvothermal method, according to the following procedure. Titanium tetraisopropoxide (TTIP,

†To whom correspondence should be addressed.
E-mail: mskang@ynu.ac.kr

99.95%, Junsei Chemical, Tokyo, Japan) was used as the titanium and ethanol as the solvent. TTIP (1.0 mol) was added to 200 mL of ethanol and stirred homogeneously for 2 h. Acetic acid was added and the pH was maintained at 3.0 for rapid hydrolysis. The final solution was stirred homogeneously and moved to an autoclave for thermal treatment. TTIP was hydrolyzed during thermal treatment at 200 °C for 8 h under a nitrogen environment at a pressure of approximately 10 atm. The resulting precipitate was washed with distilled water until pH=7.0 and then dried at 100 °C for 24 h.

The synthesized $TiO_2$ powder was examined by XRD (X-ray Diffractometer, MPD, PANalytical, Yeungnam University, Korea) with nickel-filtered CuK$\alpha$ radiation (30 kV, 30 mA) at 2$\theta$ angles ranging from 5 to 70°, a scan speed of 10 $min^{-1}$ and a time constant of 1 s. The sizes and shapes of the $TiO_2$ particles were measured by high-resolution TEM (Transmittance Electron Microscopy, H-7600, Hitachi, Yeungnam University, Korea) operated at 120 kV. The UV-visible spectra were obtained with a Cary 500 spectrometer (Varian, Yeungnam University, Korea) with a reflectance sphere over the special range of 200 to 800 nm. The surface states and electric properties of the $TiO_2$ film were determined by EFM analysis (resolution; 0.1 nm (X-Y), 0.01 nm (Z), Veeco Co., National Center for Nanomaterials Technology, Phohang, Korea).

**2. Manufacturing Dye-sensitized Solar Cell (DSSC)**

As shown in Fig. 1, to prepare the $TiO_2$ thin film, a slurry was produced by mixing 5.0 g nanometer-sized $TiO_2$ powder with 10 mL alcohol after sonication for 24 h at 1,200 W/$cm^2$. The $TiO_2$ was fabricated by twice coating onto a fluorine-doped $SnO_2$ conducting glass plate (Hartford FTO, ~30 ohm/$cm^2$, 80% transmittance the in visible region) by using a squeeze printing technique to give an approximate thickness of 10.0 μm. The film was treated by heating at 450 °C for 30 minutes to remove the alcoholic solvent. The surface modification of the $TiO_2$ film by five acids (acetic acid, formic acid, benzoic acid, pivalic acid, and ammonic acid) with carboxyl group in comparison with base compound (ammonia; $NH_3$)-modification is important. The acid concentrations were maintained at 1.0 mole, with an immersion time of 1 h. The modified thin film electrode was immersed in a $3.0\times10^{-4}$ M N719 dye solution at room temperature for 24 h, rinsed with anhydrous ethanol and dried. A Pt-coated FTO electrode was placed over the dye-adsorbed $TiO_2$ electrode, and the edges of the cell were sealed with a sealing sheet (PECHM-1, Mitsui-DuPont Poly Chemical). The redox electrolyte consisted of 0.50 mol KI, 0.05 mol $I_2$, and 0.5 mol 4-tert-butylpyridine as a solvent. Modification of the acidic or ammonia achieved a variety of colors for the acquired film electrodes. Treatment with benzoic and pivalic acids produced bright colors, whereas acetic acid and ammonia produced a dark color. This result suggested that the interaction between the $TiO_2$ film and dye molecules differed according to the variation in chemical properties induced by the surface modification. However, the formic acid modification did not induce any color change. The photocurrent-voltage (I-V) curves (Sun2000 solar simulator, ABET technology, Yeungnam University, Korea) were used to calculate the short-circuit current density ($J_{sc}$), open-circuit voltage ($V_{oc}$), fill factor (FF), and overall conversion efficiency of the DSSC. The I-V curves were measured under white light irradiation from a xenon lamp (max. 150 W, Newport). The incident light intensity and active cell area were 100 mW/$cm^2$ and 0.40 (0.8×0.5) $cm^2$,

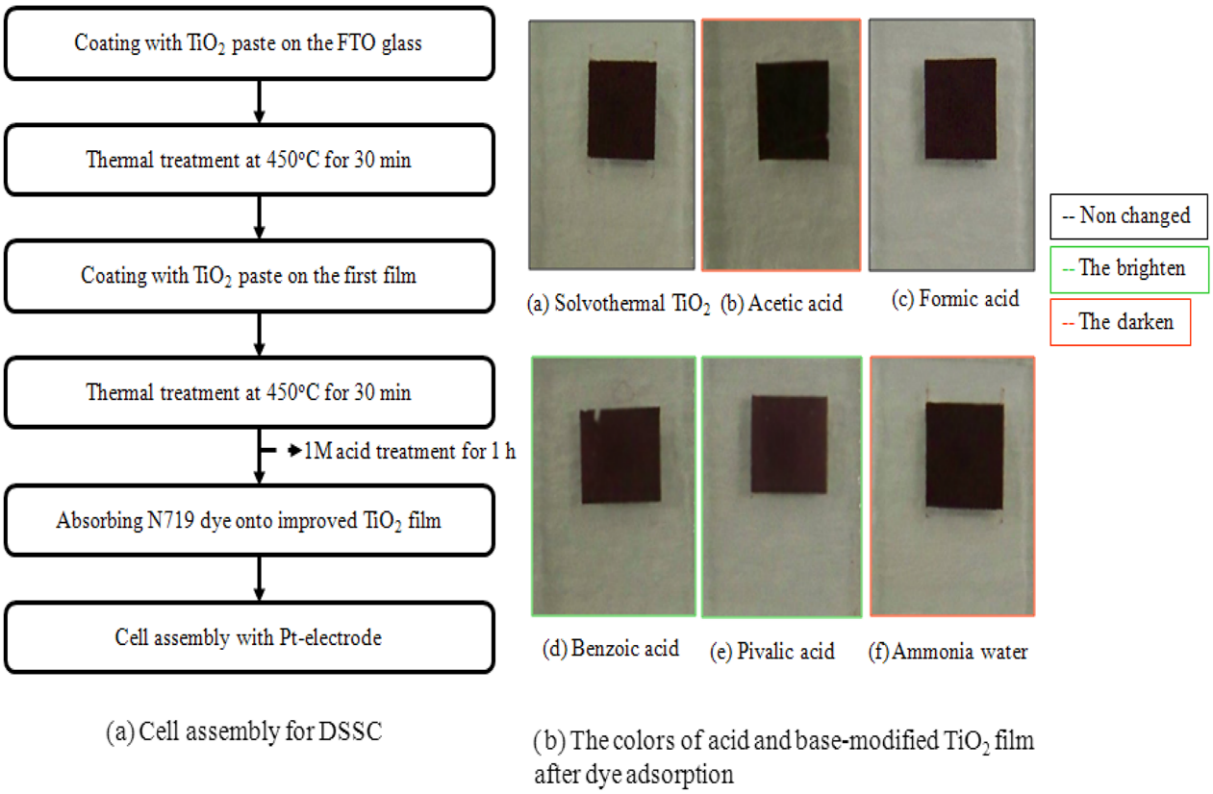


**Fig. 1. Cell assembly (a) for DSSC with modification by various acids and ammonia onto nanometer-sized $TiO_2$ prepared using the conventional solvothermal method and the colors (b) of the acid- and ammonia-modified $TiO_2$ films after dye adsorption.**

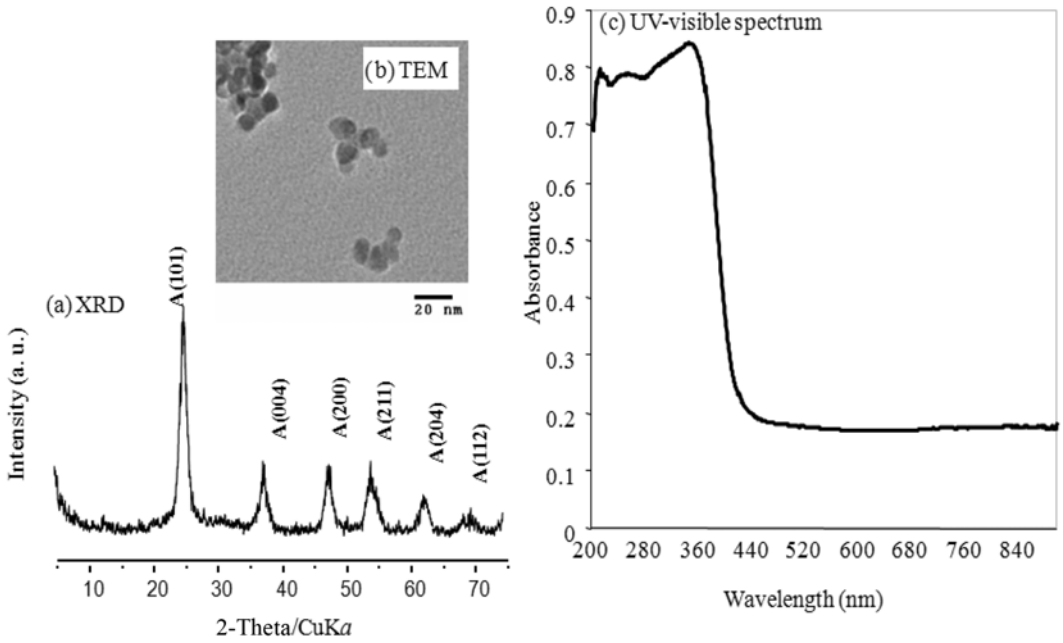


**Fig. 2. XRD pattern (a), TEM image (b), and UV-visible spectrum (c) of $TiO_2$ prepared using the conventional solvothermal method.**

respectively.

## RESULTS AND DISCUSSION

Fig. 2 shows the XRD pattern, TEM image, and UV-visible spectrum of the $TiO_2$ nanometer-sized powder prepared by the solvothermal method. The anatase structure showed peaks at 25.3, 38.0, 48.2, 54, 63, and 68° $2\theta$, which were assigned to the ($d_{101}$), ($d_{004}$), ($d_{200}$), ($d_{105}$), ($d_{211}$), and ($d_{204}$) planes, respectively [10]. The full width at half maximum (FWHM) of the peak at 25.3° $2\theta$ was 1.593°. Scherrer's equation [11], $t=0.9\lambda/\beta\cos\theta$, where $\lambda$ is the wavelength of the incident X-rays, $\beta$ the FWHM height in radians, and $\theta$ the diffraction angle, was used to estimate the crystalline domain size as 14.7 nm. The upper photos of Fig. 2 show TEM images of the particle shape of $TiO_2$. A relatively uniform mixture of rhombic and spherical particles with sizes ranging from 10 to 15 nm was observed. The UV-visible spectrum of the $TiO_2$ was obtained to determine the relationship between the solar energy conversion efficiency and spectroscopic property, as shown on the right. The absorption band for the tetrahedral symmetry of $Ti^{4+}$ normally appears at approximately

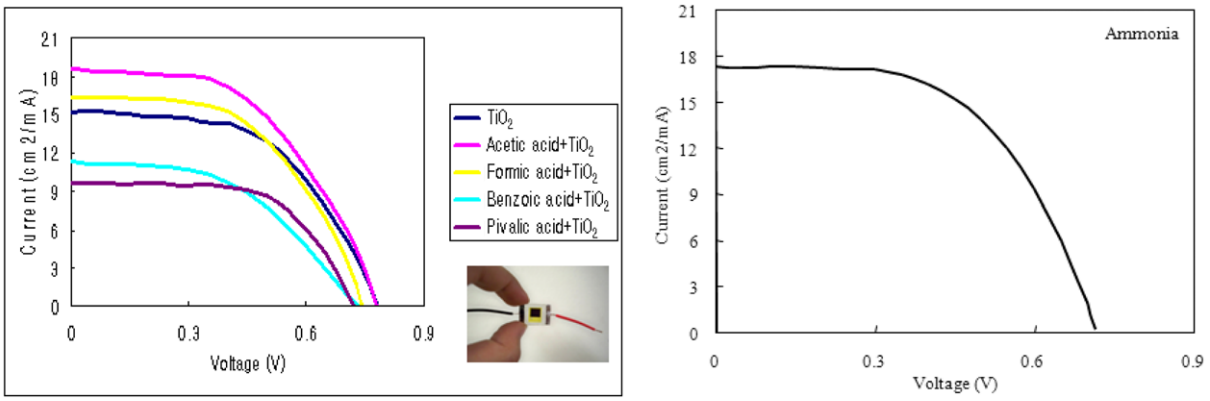


| Working electrode | Dye | Photo-efficiency (%) | Fill factor | $J_{sc}$ (mA/cm$^2$) | $V_{oc}$ (v) |
|---|---|---|---|---|---|
| $TiO_2$ | N719 | 6.25 | 0.65 | 15.15 | 0.78 |
| Acetic acid-$TiO_2$ | N719 | 7.50 | 0.65 | 18.66 | 0.77 |
| Formic acid-$TiO_2$ | N719 | 6.86 | 0.66 | 16.36 | 0.74 |
| Benzoic acid-$TiO_2$ | N719 | 4.78 | 0.64 | 11.30 | 0.73 |
| Pivalic acid-$TiO_2$ | N719 | 4.42 | 0.67 | 9.57 | 0.71 |
| Ammonia-$TiO_2$ | N719 | 7.05 | 0.69 | 17.34 | 0.71 |

**Fig. 3. The photoelectric efficiency as indicated by I-V curves in DSSC for the acid- and ammonia-modified $TiO_2$ films.**

350 nm, with strong band intensity. The band gaps in a semiconductor material are closely related to the wavelength range absorbed, where the band gap decreases with increasing absorption wavelength. In our previous report [12], we confirmed that the solvothermal modification significantly shortened the band gap of the $TiO_2$ semiconductor and showed the better photo-activity.

The photoelectric properties were measured with a voltmeter and amperemeter (Sun2000 solar simulator, ABET technology, Yeungnam University, Korea) with a variable load. The voltammeter above power failure and a lock-in amplifier were used. A 150 W illuminant Xenon lamp was employed as a radiation source at an AM-1.5 radiation angle. The intensities of light were measured using a power analyzer and thermal smart-sensor. The FF and solar energy conversion efficiency ($\eta$) are calculated using Eqs. (1) and (2), respectively [13,14].

$$\mathbf{FF}=I_{max}\times V_{max}/I_{sc}\times V_{oc} \quad (1)$$

$$\eta\,(\%)=P_{out}/P_{in}\times 100=I_{max}\times V_{max}/P_{in}\times 100=I_{sc}\times V_{oc}\times FF \quad (2)$$

Fig. 3 shows the I-V curves of six samples of $TiO_2$ modified by five acids and ammonia. The FF, $V_{oc}$, $J_{sc}$, and overall energy efficiency were determined from the equations described above. A DSSC assembled with non-modified $TiO_2$ had a $V_{oc}$ of 0.78 V and a $J_{sc}$ of 15.15 mA/cm$^2$ at an incident light intensity of 100 mW/cm$^2$. The power conversion efficiency of the non-modified $TiO_2$ anatase structure was 6.25%. The efficiencies were enhanced with the modifications of acetic acid (7.50%), formic acid (6.86%), and ammonia (7.05%), but were decreased with the modifications of benzoic acid (4.78%) and pivalic acid (4.42%), due to their three-dimensional hindrance resulting from their larger molecules, and the electron-withdrawing effect. In particular, the efficiency enhancement reached 7.50% in the DSSC made from the acetic acid-modified $TiO_2$ film, with a $J_{sc}$ of 18.66 mA/cm$^2$ and a $V_{oc}$ of 0.77 V. This result confirmed that the modified $TiO_2$ with the light- and electron-donating acids is a better material in DSSC than the non-modified $TiO_2$.

Fig. 4 shows the interfacial binding energy between the dye molecules (N719) and the surface of the modified $TiO_2$ films, which was examined by FT-IR spectroscopy. Generally, the efficiency of the charge injection process is strongly dependent on the bonding structure of the dye molecules adsorbed on the $TiO_2$ film. In addition,

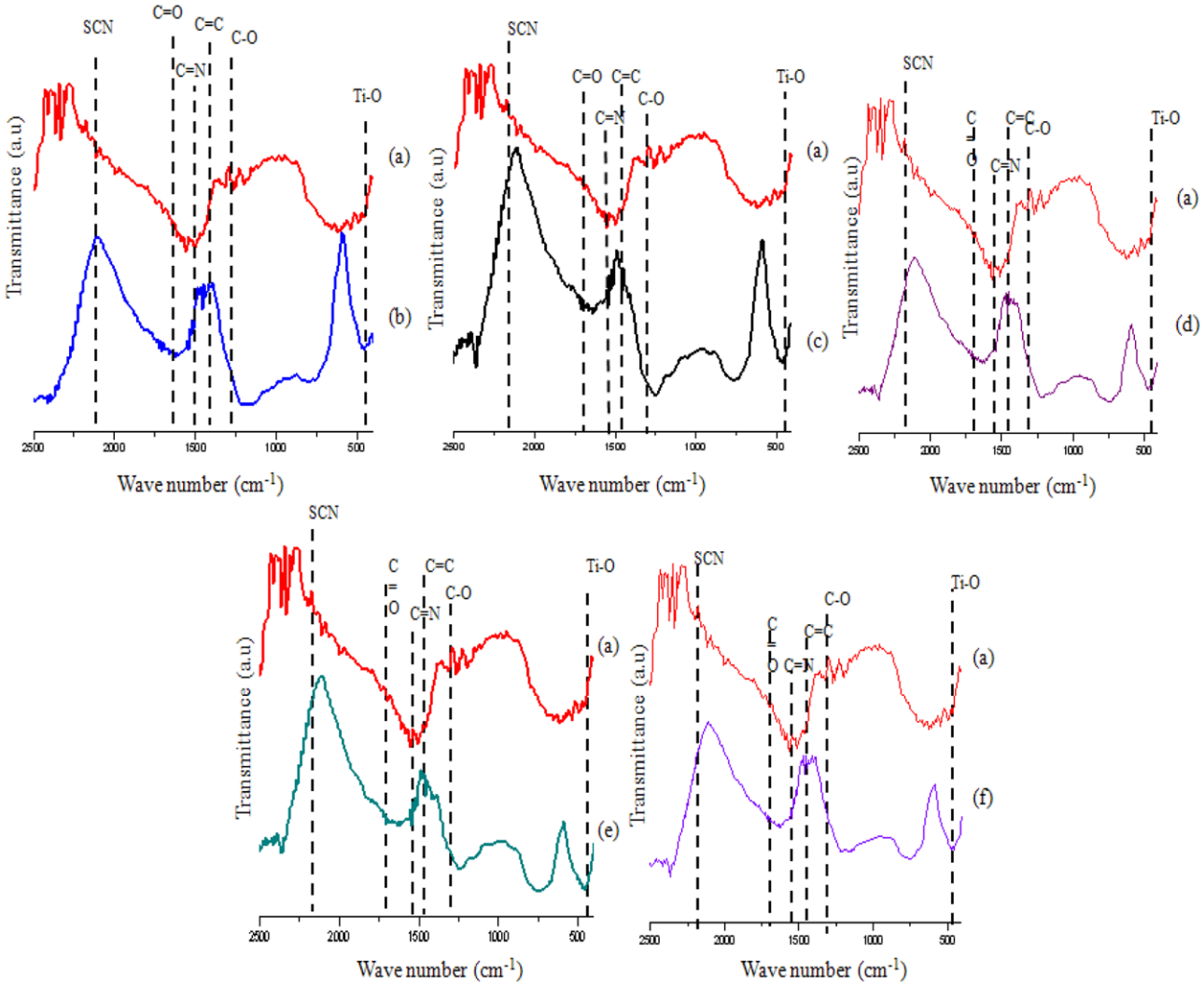


**Fig. 4. FT-IR spectra on acid and ammonia-modified $TiO_2$ films after N719 dye adsorption: (a) non-modified, (b) ammonia-modified, (c) acetic acid-modified, (d) formic acid-modified, (e) benzoic acid-modified, and (f) pivalic acid-modified $TiO_2$ films.**

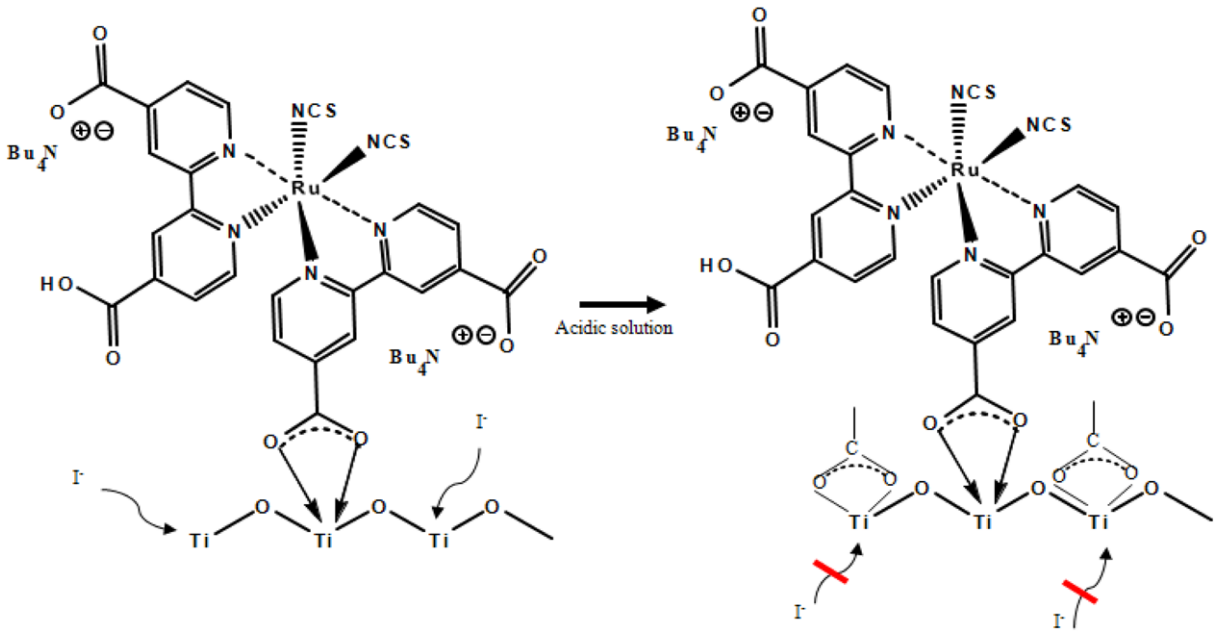


**Scheme 1. The interaction model between dye molecules and $TiO_2$ surface treated by carboxylic acidic solution.**

electron transfer in a DSSC is strongly affected by electrostatic and chemical interactions between the $TiO_2$ surface and the adsorbed dye molecules. Regarding the specific adsorption for FT-IR, the absorptions around 2,100-2,200 and 1,550 $cm^{-1}$ were assigned to the SCN and C=N stretching bonds, respectively. The IR spectra showed absorption at 1,000-1,200 and 1,610-1,650 $cm^{-1}$, which were assigned to the C-O and C=O stretching modes, respectively. For the acetic and formic acid-modified $TiO_2$ films, the C=O band was decreased but the C-O band was increased because it was transferred to the C-O stretching mode due to bidentate coordination of the N719 dye on the surface of the $TiO_2$ films. On the other hand, the C=O band was rather significant on the benzoic and pivalic acid-modified $TiO_2$ films. This suggested that coordination of the N719 dye on the non- and the benzoic and pivalic acid-modified $TiO_2$ films was mainly due to the contribution of the monodentate and partially to that of the bidentate linkage. The bond between $COO^-$ and the surface of the acetic and formic acid-modified $TiO_2$ films was assumed to be strong due to the perfect bidentate linkage. Furthermore, the IR spectrum of the acetic and formic acid-modified $TiO_2$ films showed a strong band at 500 $cm^{-1}$, which was assigned to a metal-O bond, due to the formation of a new Ti-O bond between the O of $COO^-$ and the Ti atom, which was relatively weaker in the non-modified $TiO_2$. Therefore, the acetic and formic acid-modified $TiO_2$ films had a better surface morphology than the non-modified $TiO_2$ film, resulting in an increase in $I_{sc}$ due to the transportation of electrons.

As suggested in the beginning, the most important factor for increasing the DSSC efficiency is the strong interaction between the dye and the $TiO_2$. Typically, when DSSC is driven, holes are created in the HOMO of the dye, because of electron transferring from the HOMO to the LUMO of the dye, and so the electrons move to the surface of $TiO_2$. The holes are filled again by electron of electrolyte, where the information has to be considered seriously; it prevents reduction of the $TiO_2$ surface by the electrolyte, not the dye HOMO reduction. If the surface of $TiO_2$ is reduced by the electrolyte, the $TiO_2$ surface is difficult trying to get the electrons from the dye and the conclusion is the photoelectric efficiency drop. In this study, in the DSSC cell assembly process, the $TiO_2$ photovoltaic efficiency is improved with doing the acidic treatment. We consider as shown in Scheme 1 that the $TiO_2$ surfaces, do not absorb dye, are blocked by carboxylic acid materials of small size, and the reaction between the electrolyte and the $TiO_2$ surface is depressed; however, the result is the opposite with the larger acid molecules. Consequently, interaction between the dye and the $TiO_2$ is increased relatively as a result of FT-IR.

The analytical method of EFM was used to determine the electron transfer on the different surface morphology in a higher electric current. Typically, the presence of a conductor and non-conductor within a nanometer-leveled film in the visual image can be distinguished by atomic force microscopy (AFM) using the modified EFM image. The power strength of the image between the samples and tips is measured while traversing voltage to the AFM tip bias. The presence of conducting and non-conducting areas in the sample can be determined from the responses of the AFM tip. [15] The phase changes periodically with the tip vibrating power cycle according to the charge and magnetic orientation. Consequently, the differences between the conducting and non-conducting surfaces are indicated by the amplitude and phase changes, and the change in width is expressed as the contrast of the image and roughness values (Ra). An Ra value in the phase is represented by the electrostatic field gradient. Therefore, the larger Ra value severely when tips specific in many areas of current are used. The Ra value can be determined indirectly by changing the twitch of the tip, according to the following equation [16,17].

$$Ra = 1/L_x L_y \int_0^{Ly} \int_0^{Lx} |f(x,y)| dx\ dy$$

Where f(x, y) is the surface relative to the center plane and $L_x$ and

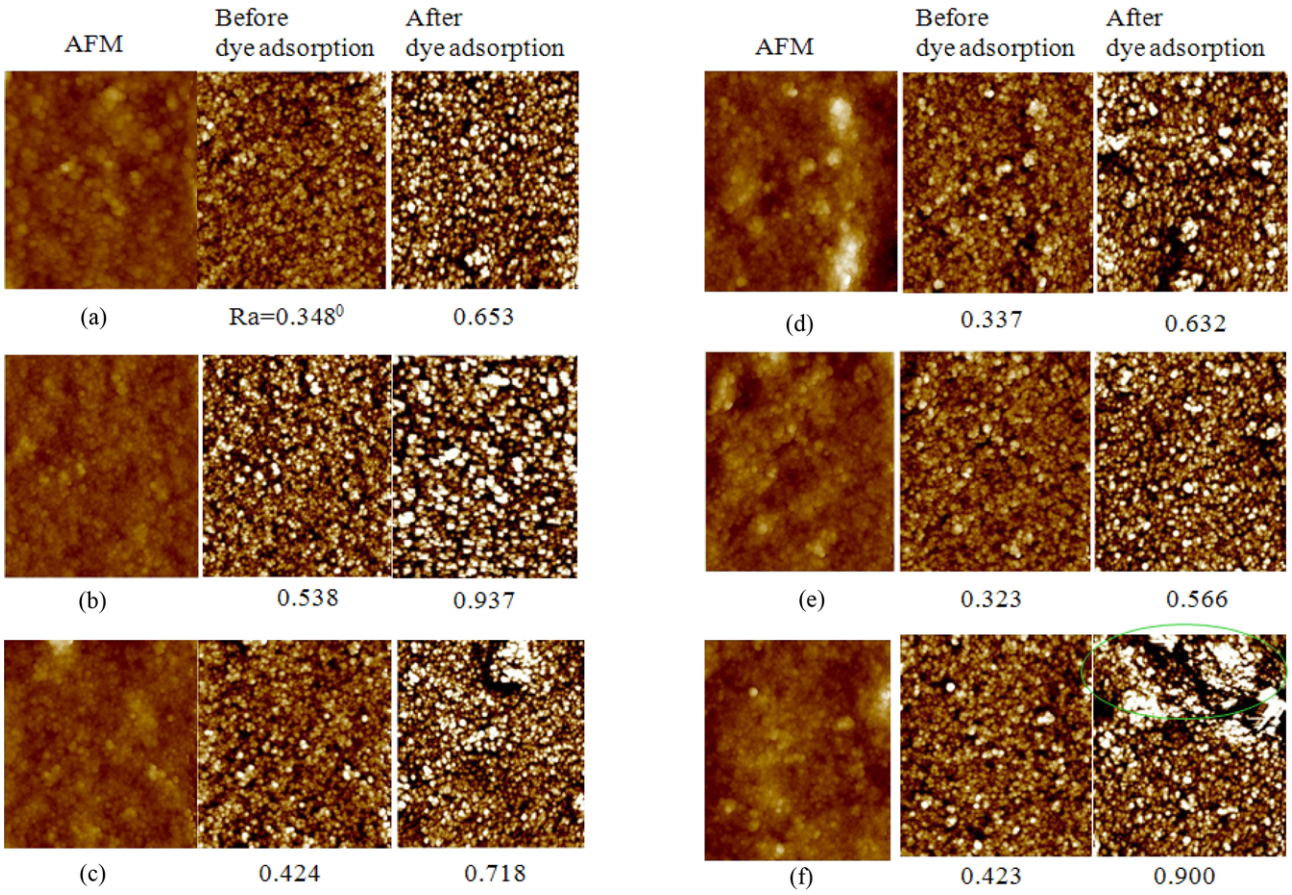


**Fig. 5. AFM and EFM images of non- and acid-modified $TiO_2$ with and without N719dye adsorption: (a) non-modified, (b) acetic acid-modified, (c) formic acid-modified, (d) benzoic acid-modified, (e) pivalic acid-modified, and (f) ammonia-modified $TiO_2$ films.**

$L_y$ are the dimensions of the surface.

Fig. 5 shows AFM and EFM images of six types of $TiO_2$ film before and after absorption of N719 dye in light condition. All $TiO_2$ films were 4.0 μm thick. When traversing at a voltage of 3.0 eV, the phase change was a maximum of 3.0 degrees in both samples. The phase difference is the difference in electrostatic force between phases, so that a bright image in the figure generally indicates the flow of charge [18]. When the five types of modified $TiO_2$ film were measured under light conditions, the images in the EFM photos were brighter than in the AFM photos, and in particular, the images were brighter with the adsorbing dye. The acetic and formic acid-modified $TiO_2$ films showed a more significant result after the adsorbing dye compared to the non-, and the benzoic and pivalic acid-modified $TiO_2$ films. In the ammonic acid modification, unfortunately, the $TiO_2$ particles were exfoliated from the FTO surface, indicating that the effectiveness of the ammonia-modification was only temporary, and that this effectiveness would decrease long-term. Fig. 5 also shows the averaged Ra value of the six types of $TiO_2$ film, with and without dye adsorption, in the light condition. The non-modified $TiO_2$ film did not have a significant value before dye adsorption, but The Ra value was increased by 0.348 degrees from 0 degrees for the non-modified $TiO_2$ film before dye adsorption to 0.653 degrees after dye adsorption. Otherwise, the Ra value in the acetic acid-modified $TiO_2$ film was 0.937, which was 1.5-fold greater than that of the non-modified sample. These results revealed the good mobility of the electrons flowing onto the surface of the $TiO_2$ film modified with the five types of acid, especially acetic acid.

## CONCLUSION

Nanometer-sized $TiO_2$ was modified by using five acids in a cell assembly procedure to enhance the solar energy conversion efficiency. The performance on non-modified $TiO_2$ film in DSSC was compared with those of the five modified $TiO_2$ films. The acetic acid-modified $TiO_2$ DSSC showed excellent solar energy conversion efficiency compared to that of the non-modified $TiO_2$ and of that modified by the other four acids. In 100 $mW/cm^2$ simulated sunlight, the performance of the acetic acid-modified $TiO_2$ DSSC was as follows: solar energy conversion efficiency=7.50%, $V_{oc}$=0.77 V, $J_{sc}$=18.66 $mA/cm^2$, and FF=0.66. The electron density and electron flow on the DSSC films were explained by using roughness analysis based on the EFM images. Electrons were transferred more rapidly to the surface of the acetic acid-modified $TiO_2$ film than in the case of the non-modified $TiO_2$ film. Additionally, the FT-IR analysis results indicated that the interaction between the $TiO_2$ surface and dye molecules was strengthened by the acetic acid modification.

## ACKNOWLEDGEMENT

This research was supported by the Basic Science Program through

the National Research Foundation of Korea (NRF) funded by Ministry of Education, Science and Technology (2009-0064865), for which the authors are very grateful.

## REFERENCES

1. A. W. Blakers and T. Armour, *Sol. Cells*, **93**, 1440 (2009).
2. Y. Wang, Z. Fang, Li. Zhu, Q. Huang, Y. Zhang and Z. Zhang, *Appl. Energy*, **86**, 1037 (2009).
3. P. N. Vinod, *Solid State Commun.*, **149**, 957 (2009).
4. P. Li, P, Wua and J. Lin, *J. Sol. Energy*, **83**, 845 (2009).
5. N. H. Rajesh, R. H. Ragunatharaddi and T. N. Sharanappa, *Colloids & Surface B*, **72**, 259 (2009).
6. S. Gagliardi, L. Giorgi, R. Giorgi, N. Lisi, Th. Makris, E. Salernitano and A. Rufoloni, *Superlattices & Microst.*, **46**, 205 (2009).
7. R. Lee and Y. Huang, *Thin Solid Films*, **517**, 5903 (2009).
8. C. S. Chou, R. Y. Yang, C. K. Yeh and Y. Lin, *J. Powder Technol.*, **194**, 95 (2009).
9. J. H. Park, K. J. Choi and S. Kang, *J. Power Sources*, **183**, 812 (2008).
10. R. Dholam, N. Patel and M. Adami, *Inter. J. Hydrogen Energy*, **33**, 6896 (2008).
11. H. P. Klug and L. F. Alexander, About Tachyons, *Phys. Today*, 2Ed, John Wiley & Sons, Inc., 716 (1954).
12. Y. Kim, J. Lee, H. Jeong, Y. Lee, M. Um, K. M. Jeong, M. Yeo and M. Kang, *J. Ind. Eng. Chem.*, **14**, 396 (2008).
13. M. Gratzel, *J. Photochem. Photobiol.*, **4**, 145 (2003).
14. K. Kalyanasundaran and M. Gratzel, *Coordination Chem. Reviews*, **177**, 347 (1999).
15. F. M. Serry, K. Kjoller and T. Thorntin, Scanning Probe Microscopy, Veeco Instruments Inc. (2007).
16. T. V. Vorburger, J. A. Dagata, G. Wilkening and A. W. Czanderna, *Beam Effects, Surface Topography, and Depth Profiling in Surface Analysis*, Edited by Czanderna et al., Plenum Press, New York (1998).
17. H. Sun, Z. Li, J. Zhou, Y. Zhao and M. Lu, *Surf. Sci.*, **253**, 6109 (2007).
18. P. Girard, *Phys. Puv. Nanotech.*, **12**, 485 (2001).